ChemComm

COMMUNICATION

View Article Online
View Journal | View Issue

Cite this: *Chem. Commun.*, 2023, 59, 10608

Received 13th July 2023,
Accepted 1st August 2023

DOI: 10.1039/d3cc03387b

rsc.li/chemcomm

Towards the quantification of the chemical mechanism of light-driven water splitting on GaN photoelectrodes

Artem Shushanian, [a] Daisuke Iida, [b] Yu Han [a] and Kazuhiro Ohkawa *[b]

We present results from a study addressing the unbiased water-splitting process and its side reactions on GaN-based photoelectrodes decorated with NiO_x, FeO_x, and CoO_x nanoparticles. Observations involving physicochemical analyses of liquid and vapour phases after the experiments were performed in 1 M NaOH under ambient conditions. A water-splitting process with GaN-based photoelectrodes results in the generation of hydrogen gas and hydrogen peroxide. Quantification of the water-splitting chemical mechanism gave numerical values indicating an increase in the device performance and restriction of the GaN electrocorrosion with surface modifications of GaN structures. The hydrogen generation efficiencies are η_{H_2}(bare GaN) = 1.23%, η_{H_2}(NiO_x/GaN) = 4.31%, η_{H_2}(FeO_x/GaN) = 2.69%, and η_{H_2}(CoO_x/GaN) = 2.31%. The photoelectrode etching reaction moieties Q_{etch}/Q are 11.5%. 0.21%, 0.26% and 0.20% for bare GaN, NiO_x/GaN, FeO_x/GaN, and CoO_x/GaN, respectively.

Storage of solar energy in chemical bonds is a suitable route towards diversification of mass production of essential substances in industry. Application of III-nitride materials offers the possibility of light-driven splitting of the water to hydrogen gas and products of water oxidation.[1] In addition to the intrinsic thermal and chemical stability of III-nitrides,[2–6] they show a tendency to enhance their performances and durability when modified with nanoparticles (NPs) based on transition metal oxides[7–10] and noble metals,[11–13] and their combinations.[14–16]

The lifetime of III-nitride-based photoanodes varies with different NP materials and deposition techniques, so we need to study the reaction products to quantify the decrease in the electrode etching. Also, we expect to clarify the amounts of anodic water oxidation products as the oxygen gas is the only product that has previously been reported.[7,9,11,17,18] Due to the significant impact of transition metal oxide NPs on the properties of the water-splitting process on III-nitrides, we suggest measuring their dissolution rates.

In this work, we present an approach to quantifying the water-splitting process and its corresponding side reactions on GaN-based photoelectrodes (Table 1). We observed that ultraviolet (UV)-light-driven reactions on bare GaN, NiO_x/GaN, FeO_x/GaN, and CoO_x/GaN structures form the basis for further studies on the processes driven by visible light on III-nitride alloys and can help select the optimal surface modification of III-nitride-based devices for water splitting.

Fig. 1a represents the photocurrent generated as a result of zero-bias UV irradiation of GaN-based structures in 1 M NaOH solution with the Pt counterelectrode in a configuration shown in Fig. 1b. NiO_x decorated structures provided the highest reaction current ($\sim$3.0 mA), and samples with FeO_x and CoO_x NPs showed lower currents of 1.5 and 1.3 mA, respectively. The bare GaN photoelectrode provided the lowest reaction current of $\sim$0.7 mA. We calculated the total charges of reactions Q (C) *via* integration of current evolutions I (A) with the exposition time t (s), as shown in eqn (1):

$$Q = \int_0^t I\,\mathrm{d}t \tag{1}$$

We observed vigorous generation of gas at the Pt counterelectrode side during the experiments. The amounts of hydrogen closely corresponded to the total charges registered. Several bubbles of gas were observed at the working electrode side; however, there was not enough gas present there to register.

In our previous studies on n-GaN etching, we found hydrogen peroxide (H_2O_2) to be a major product of water oxidation, so we expected the photoelectrode to generate peroxides as a main product of the water splitting reaction.[21,22] Theoretical investigations of the water-splitting process on the GaN surface propose the dimerization of hydroxyl species during oxygen generation.[23,24] Also, the studies on water splitting with carbon nitride photoelectrodes report the generation of hydrogen peroxide.[25–28] To quantify the amounts of peroxide formed,

[a] *Chemistry Program, Physical Science and Engineering Division King Abdullah University of Science and Technology (KAUST), Thuwal 23955-6900, Kingdom of Saudi Arabia. E-mail: kazuhiro.ohkawa@kaust.edu.sa*
[b] *Electrical and Computer Engineering Program, Computer, Electrical and Mathematical Sciences and Engineering Division King Abdullah University of Science and Technology (KAUST), Thuwal 23955-6900, Kingdom of Saudi Arabia*

Table 1 Observations of zero-biased light-driven water splitting on GaN-based structures in the literature

Photoanode	NPs	Electrolyte	Product analysis		Year[Ref.]
			Gas	Liquid	
GaN	None	1 M KOH	±[a]	–	2005[1]
Patterned GaN	None	1–5 M NaOH	±	–	2007[19]
GaN powder	None, RuO_2, $Rh_{2y}Cr_yO_x$	2.4 M MeOH, 0.01 M $AgNO_3$	+	–	2007[20]
GaN nanowires	Pt	1 M H_2SO_4	+	–	2017[11]
GaN, β-Ga_2O_3/GaN	$Ni_3(PO_4)_2$	0.5 M NaOH	+	–	2022[17]
GaN	Au	1 M NaOH	–	–	2022[12]
GaN	None, FeO_x, CoO_x, NiO_x	1 M NaOH	+	+	This work

[a] Only the generation of H_2 is mentioned.

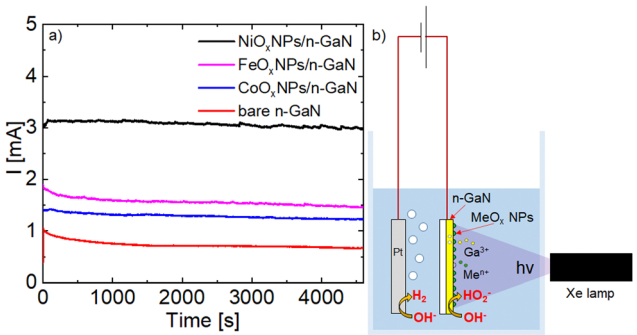

Fig. 1 (a) Photocurrents of water splitting reactions on n-GaN-based structures. The values are normalized to 1 cm^2 of photoelectrode area, and (b) schematic representation of the experimental configuration.

we used the iodine reverse titration in acidic media. Hydrogen gas and the hydrogen peroxide generation efficiencies (η_{H_2} and $\eta_{H_2O_2}$) were calculated according to the following equation (eqn (2) and Table 2):

$$\eta_{H_2} = \frac{n_{H_2}\Delta G}{P_0 t}; \quad \eta_{H_2O_2} = \frac{n_{H_2O_2}\Delta G}{P_0 t} \tag{2}$$

in which n_{H_2} (mol) and $n_{H_2O_2}$ (mol) are the amounts of generated hydrogen gas and hydrogen peroxide, respectively, ΔG (354 kJ mol^{-1}) is Gibbs free energy of water splitting to H_2 and H_2O_2, P_0 (100 mW cm^{-2}) is the light power density, and t (s) is the exposition time.

We quantitatively characterized the water-splitting reaction by identifying hydrogen gas at the cathode and peroxides in the electrolyte. In this situation, we assumed that a two-electron water oxidation occurred that resulted in the products we observed. Hydroxide anions were reduced to hydroxide anions on a working electrode side (eqn (3)):

$$3OH^- \rightarrow HO_2^- + H_2O + 2e^- \tag{3}$$

Table 2 Total reaction charges, amounts of generated products and their generation efficiencies

Photoelectrode	Q (C)	n_{H_2} (mol)	$n_{H_2O_2}$ (mol)	η_{H_2} (%)	$\eta_{H_2O_2}$ (%)
Bare GaN	3.3	1.6×10^{-5}	1.4×10^{-5}	1.23	1.08
NiO_xNPs/GaN	14.1	5.6×10^{-5}	5.5×10^{-5}	4.31	4.23
FeO_xNPs/GaN	7.2	3.5×10^{-5}	3.3×10^{-5}	2.69	2.54
CoO_xNPs/GaN	5.9	3.0×10^{-5}	2.9×10^{-5}	2.31	2.23

Also, we supposed a four-electron water oxidation process that resulted in the generation of the oxygen gas, which occurred as a side reaction on the photoelectrode (eqn (4)):

$$4OH^- \rightarrow O_2 + 2H_2O + 4e^- \tag{4}$$

Both water oxidation and GaN etching processes led to the generation of hydrogen gas on the cathode (eqn (5)):

$$2H_2O + 2e^- \rightarrow H_2 + 2OH^- \tag{5}$$

The charge of the reaction responsible for the etching of GaN (Q_{etch}) was calculated in agreement with our previous investigation of electrooxidation of GaN in which we proved this process to be a system of six-electron reactions (eqn (6)):[21,22]

$$Q_{etch} = 6F(n_{Ga} - n_{Ga\,BG}) \tag{6}$$

in which F is Faraday's constant (96 485 C mol^{-1}), n_{Ga} (mol) is the concentration of Ga in the electrolyte after the experiment, and $n_{Ga\,BG}$ (mol) is a background concentration of Ga, measured after the storage of the similar samples in 1 M NaOH for 4600 s without UV-light irradiation. We assume that threading dislocations propagating through the whole thickness of the GaN structures provide channels for access of the n-GaN layer to the electrolyte.[29] As the reaction current remained relatively constant within the exposition time, we consider that the etching of GaN takes the same moiety of the total charge of the water-splitting process. Modification of the GaN structures with CoO_x resulted in the lowest moiety of the charge spent on the electrooxidation of the GaN photoelectrode.

Table 3 shows the results of the inductively coupled plasma-mass spectrometry (ICP-MS) measurements of the electrolytes after keeping the samples that were exposed or not exposed to UV light. When the light was off, GaN hardly dissolved in 1 M NaOH; however, the decoration of its surface with oxide NPs limited this process. Coating the GaN structures with oxide NP produced an increase in the water splitting reaction rate and slowed the corrosion of GaN as shown before.[30] In this study, we observed the highest reaction rate for the sample modified with NiO_x NPs, while the concentrations of Ni after both experiments with and without UV light exposure were higher than the concentrations of other metals in the electrolyte after the corresponding experiments on FeO_x/GaN and CoO_x/GaN. The highest inhibition of the GaN electrooxidation reaction was observed for the CoO_x/GaN system where the concentrations of

Table 3 Concentrations of metal ions in the electrolytes and charges of GaN etching reactions

Photoelectrode	n_{Ga} (mol)	n_{Me}[a] (mol)	$n_{Ga\,BG}$ (mol)	$n_{Me\,BG}$[b] (mol)	Q_{etch} (C)	Q_{etch}/Q (%)
Bare GaN	7.3×10^{-7}	<LOD[c]	7.1×10^{-8}	<LOD	0.38	11.5
NiO_xNPs/GaN	5.8×10^{-8}	1.1×10^{-6}	7.0×10^{-9}	6.9×10^{-8}	0.030	0.21
FeO_xNPs/GaN	3.7×10^{-8}	6.1×10^{-7}	4.0×10^{-9}	4.7×10^{-8}	0.019	0.26
CoO_xNPs/GaN	2.3×10^{-8}	2.3×10^{-7}	2.2×10^{-9}	9.0×10^{-9}	0.012	0.20

[a] Corresponding metal (Ni, Fe, or Co) concentration after the water-splitting experiment driven by UV light on the MeO_xNPs/GaN photoelectrode. [b] Corresponding metal (Ni, Fe, or Co) background concentrations, measured after storing the MeO_xNPs/GaN photoelectrode in the electrolyte with no exposure to UV light. [c] Limit of detection.

Co are the lowest after the experiments with and without UV light. In agreement with the calculated values of Q_{etch}/Q, the introduction of metal oxide NPs potentially increases the durability of the GaN photoelectrodes by 54.8 times with the NiO_x NPs, by 44.2 times with the FeO_x NPs, and by 57.5 times with the CoO_x NPs.

Observations on the concentrations of the metals after the experiment show the involvement of the oxide NPs in the process. Thus, we observed several processes on MeO_x/GaN that run under UV irradiation: (1) water splitting to hydrogen gas and peroxides, (2) electrooxidation of GaN described, and (3) interactions of metal oxides with the reaction layers. We quantitatively proved that inhibition of the GaN etching reaction *via* modification of the GaN structures with metal oxide NPs occurs.

In summary, we presented the water-splitting process on bare GaN, NiO_x/GaN, FeO_x/GaN, and CoO_x/GaN structures. Introduction of the NiO_x NPs shows the highest increase in reaction rate while the CoO_x NPs provide the highest durability of the GaN-based devices. The major product of the water splitting on GaN structures is a result of the two-electron decomposition of water to hydrogen peroxide and hydrogen gas. Our approach may help optimize modifications of the III-nitride-based photoelectrodes in the future. A detailed understanding of the mechanisms of water oxidation reactions and the side processes would clarify the possibility of effective solar energy storage in commercially valuable chemical products.

The working electrode was a thin film structure (top to bottom) with unintentionally doped (uid)-GaN (100 nm, $n \approx$ mid. 10^{16} cm^{-3})/Si-doped n-GaN (3 μm, $n = 3 \times 10^{18}$ cm^{-3})/uid-GaN (2 μm, $n \approx$ mid. 10^{16} cm^{-3}), grown using the metalorganic vapour-phase epitaxy method on patterned *c*-plane sapphire. We decorated the top layer with spin-coated and annealed MeO_x NPs described elsewhere for Me = Co[8] and Me = Ni, Fe.[9] We ran the experiments on a light-driven water-splitting apparatus for 4600 s in a two-electrode configuration in which a Pt wire was used as a counter electrode with no applied electrical bias. A Xe arc lamp (300 W) filtered with a UV spectroscopic mirror irradiated the surface of the working electrodes with the power density of 100 mW cm^{-2}. We used a 1 M NaOH solution prepared by dissolving NaOH (Fisher Scientific, ≥97.5% [w/w%]) in deionized water (MilliQ) as an electrolyte in our experiments.

Light-driven water splitting on GaN resulted in the generation of products in both liquid and vapour phases. We collected vapour phase products near the electrodes and analyzed them using a gas chromatograph (Shimadzu GC-8A). To measure the concentrations of metals in the electrolyte after the experiment, we used ICP-MS (Thermo iCAP). Relative standard deviations for the calibrations were 7.7% for ^{56}Fe and 3.4% for ^{57}Fe in kinetic energy distribution (KED) mode, 3.1% (KED) and 2.8% (standard mode) for ^{59}Co, 0.8% (KED) and 2.5% (standard) for ^{60}Ni, 0.4% (KED) and 10.6 (standard) for ^{62}Ni, 0.6% (KED) and 1.3% (standard) for ^{69}Ga, and 1.5% (KED) and 0.8% (standard) for ^{71}Ga. The background concentrations of these metals were calculated after the storage of the similar samples in the electrolyte with no UV irradiation for 4600 s. We used ^{103}Rh as an internal standard for ICP-MS measurements. We found and quantified the peroxide amounts by carefully diluting our aliquots with sulfuric acid (Fisher Scientific, 95.0 to 98.0% [w/w%]) and application of iodine reverse titration with potassium iodide (Fluka, Z99% [w/w%]) and sodium thiosulfate pentahydrate (Fisher Scientific, 99.5 to 101.0% [w/w%]) solutions.

We normalized the reaction currents, generated gas volumes, peroxide, and metal concentrations to 1 cm^2 of irradiated GaN photoelectrodes for the correct comparison and analysis.

A. S.: investigation, methodology, writing – original draft; D. I.: validation, writing – review & editing; Y. H.: supervision, writing – review & editing; K. O.: conceptualization, project administration, writing – review & editing.

This work was financially supported by King Abdullah University of Science and Technology (KAUST) (BAS/1/1676-01-01). We would like to show our gratitude to the staff of the KAUST Analytical Core Lab, in particular Andrei Zybinskii, for their help with the ICP-MS calibration and measurements.

Conflicts of interest

There are no conflicts to declare.

Notes and references

1 K. Fujii, T. Karasawa and K. Ohkawa, *Jpn. J. Appl. Phys.*, 2005, **44**, L543.
2 F. Medjdoub, J.-F. Carlin, M. Gonschorek, E. Feltin, M. A. Py, D. Ducatteau, C. Gaquiere, N. Grandjean and E. Kohn, *2006 International Electron Devices Meeting*, IEEE, 2006, pp. 1–4.
3 B. Imer, F. Wu, M. D. Craven, J. S. Speck and S. P. DenBaars, *Jpn. J. Appl. Phys.*, 2006, **45**, 8644.
4 D. Maier, M. Alomari, N. Grandjean, J.-F. Carlin, M.-A. Diforte-Poisson, C. Dua, A. Chuvilin, D. Troadec, C. Gaquière, U. Kaiser, S. L. Delage and E. Kohn, *IEEE Trans. Device Mater. Reliab.*, 2010, **10**, 427–436.
5 S. Chen and L.-W. Wang, *Chem. Mater.*, 2012, **24**, 3659–3666.
6 A. R. Acharya, *Himalayan Phys.*, 2014, **5**, 22–26.
7 T. Hayashi, M. Deura and K. Ohkawa, *Jpn. J. Appl. Phys.*, 2012, **51**, 112601.
8 M. Velazquez-Rizo, D. Iida and K. Ohkawa, *Jpn. J. Appl. Phys.*, 2019, **58**, SCCC23.
9 M. Velazquez-Rizo, D. Iida and K. Ohkawa, *Sci. Rep.*, 2020, **10**, 12586.

10 C. W. Lee, F.-W. Lin, P.-H. Liao, M.-L. Lee and J.-K. Sheu, *J. Phys. Chem. C*, 2021, **125**, 16776–16783.
11 P. Varadhan, H.-C. Fu, D. Priante, J. R. D. Retamal, C. Zhao, M. Ebaid, T. K. Ng, I. Ajia, S. Mitra, I. S. Roqan, B. S. Ooi and J.-H. He, *Nano Lett.*, 2017, **17**, 1520–1528.
12 A. Abdullah, M. A. Johar, A. Waseem, I. V. Bagal, M. A. Hassan, J. K. Lee and S.-W. Ryu, *Mater. Sci. Eng., B*, 2022, **275**, 115514.
13 Z. Li, R. Li, H. Jing, J. Xiao, H. Xie, F. Hong, N. Ta, X. Zhang, J. Zhu and C. Li, *Nat. Catal.*, 2023, **6**, 80–88.
14 K. Maeda, N. Sakamoto, T. Ikeda, H. Ohtsuka, A. Xiong, D. Lu, M. Kanehara, T. Teranishi and K. Domen, *Chem. – Eur. J.*, 2010, **16**, 7750–7759.
15 M. G. Kibria, H. P. Nguyen, K. Cui, S. Zhao, D. Liu, H. Guo, M. L. Trudeau, S. Paradis, A.-R. Hakima and Z. Mi, *ACS Nano*, 2013, **7**, 7886–7893.
16 H. N. Nong, L. Gan, E. Willinger, D. Teschner and P. Strasser, *Chem. Sci.*, 2014, **5**, 2955–2963.
17 M. Arunachalam, K. R. Subhash, K. S. Ahn, C. S. Kim, J. S. Ha, S. W. Ryu and S. H. Kang, *ACS Appl. Energy Mater.*, 2022, **5**, 2169–2183.
18 T. Sekimoto, H. Hashiba, S. Shinagawa, Y. Uetake, M. Deguchi, S. Yotsuhashi and K. Ohkawa, *Jpn. J. Appl. Phys.*, 2016, **55**, 88004.
19 I. Waki, D. Cohen, R. Lal, U. Mishra, S. P. DenBaars and S. Nakamura, *Appl. Phys. Lett.*, 2007, **91**, 93519.
20 K. Maeda, K. Teramura, N. Saito, Y. Inoue and K. Domen, *Bull. Chem. Soc. Jpn.*, 2007, **80**, 1004–1010.
21 A. Shushanian, D. Iida, Z. Zhuang, Y. Han and K. Ohkawa, *RSC Adv.*, 2022, **12**, 4648–4655.
22 A. Shushanian, D. Iida, Y. Han and K. Ohkawa, *New J. Chem.*, 2022, **46**, 23013–23018.
23 J. Wang, L. S. Pedroza, A. Poissier and M. Fernández-Serra, *J. Phys. Chem. C*, 2012, **116**, 14382–14389.
24 A. V. Akimov, J. T. Muckerman and O. V. Prezhdo, *J. Am. Chem. Soc.*, 2013, **135**, 8682–8691.
25 Y. Kofuji, Y. Isobe, Y. Shiraishi, H. Sakamoto, S. Tanaka, S. Ichikawa and T. Hirai, *J. Am. Chem. Soc.*, 2016, **138**, 10019–10025.
26 Y. Kofuji, S. Ohkita, Y. Shiraishi, H. Sakamoto, S. Ichikawa, S. Tanaka and T. Hirai, *ACS Sustainable Chem. Eng.*, 2017, **5**, 6478–6485.
27 B. Yan, Z. Chen and Y. Xu, *Chem. - Asian J.*, 2020, **15**, 2329–2340.
28 J. Chen, N. Kang, J. Fan, C. Lu and K. Lv, *Mater. Today Chem.*, 2022, **26**, 101028.
29 F. C. P. Massabuau, P. H. Griffin, H. P. Springbett, Y. Liu, R. V. Kumar, T. Zhu and R. A. Oliver, *APL Mater.*, 2020, **8**, 8–13.
30 W. Ohara, D. Uchida, T. Hayashi, M. Deura and K. Ohkawa, *Mater. Res. Soc. Symp. Proc.*, 2012, **1446**, 1–5.